HHS Public Access

Author manuscript

J Nucl Med. Author manuscript; available in PMC 2017 January 18.

Published in final edited form as:

J Nucl Med. 2016 January ; 57(1): 9–14. doi:10.2967/jnumed.115.165316.

^{68}Ga-NOTA-Aca-BBN(7–14) PET/CT in Healthy Volunteers and Glioma Patients

Jingjing Zhang[*,1,2], **Deling Li**[*,3], **Lixin Lang**[2], **Zhaohui Zhu**[1], **Ling Wang**[1], **Peilin Wu**[1], **Gang Niu**[2], **Fang Li**[1], and **Xiaoyuan Chen**[2]

[1]Department of Nuclear Medicine, Peking Union Medical College Hospital, Chinese Academy of Medical Sciences and Peking Union Medical College, Beijing, China [2]Laboratory of Molecular Imaging and Nanomedicine, National Institute of Biomedical Imaging and Bioengineering, National Institutes of Health, Bethesda, Maryland [3]Department of Neurosurgery, Beijing Tiantan Hospital, Capital Medical University, Beijing, China

Abstract

This work was designed to study the safety, biodistribution, and radiation dosimetry of a gastrin-releasing peptide receptor (GRPR)– targeting, ^{68}Ga-labeled bombesin (BBN) peptide derivative PET tracer, NOTA-Aca-BBN(7–14) (denoted as ^{68}Ga-BBN) in healthy volunteers and to assess the level of receptor expression in glioma patients.

Methods—Four healthy volunteers (2 male and 2 female) underwent whole-body PET/CT at multiple time points after a bolus injection of ^{68}Ga-BBN (111 ± 148 MBq). Regions of interest were drawn manually over major organs, and time–activity curves were obtained. Dosimetry was calculated using the OLINDA/EXM software. Twelve patients with glioma diagnosed by contrast-enhanced MRI underwent PET/CT at 30–45 min after ^{68}Ga-BBN injection. Within 1 wk afterward, the tumor was surgically removed and immunohistochemical staining of tumor samples against GRPR was performed and correlated with the PET/CT results.

Results—^{68}Ga-BBN was well tolerated in all healthy volunteers, with no adverse symptoms being noticed or reported. ^{68}Ga-BBN cleared rapidly from the circulation and was excreted mainly through the kidneys and urinary tract. The total effective dose equivalent and effective dose were 0.0335 ± 0.0079 and 0.0276 ± 0.0066 mSv/MBq, respectively. In glioma patients, all MRI-identified lesions showed high signal intensity on ^{68}Ga-BBN PET/CT. SUV_{max} and SUV_{mean} were 2.08 ± 0.58 and 1.32 ± 0.37, respectively. With normal brain tissue as background, tumor-to-background ratios were 24.0 ± 8.85 and 13.4 ± 4.54 based on SUV_{max} and SUV_{mean}, respectively. The immunohistochemical staining confirmed a positive correlation between SUV and GRPR expression level ($r^2 = 0.71$, $P < 0.001$).

For correspondence or reprints contact either of the following: Fang Li, Department of Nuclear Medicine, Peking Union Medical College Hospital, Chinese Academy of Medical Sciences, Beijing 100730, China. lifang@pumch.cn, Xiaoyuan Chen, National Institutes of Health, 35A Convent Dr., GD937, Bethesda, MD 20892. shawn.chen@nih.gov.

*Contributed equally to this work.

Conclusion—^{68}Ga-BBN is a PET tracer with favorable pharmacokinetics and a favorable dosimetry profile. It has the potential to evaluate GRPR expression in glioma patients and guide GRPR-targeted therapy of glioma.

Keywords

BBN peptide; gastrin-releasing peptide receptor (GRPR); ^{68}Ga-BBN; PET/CT; glioma

Gastrin-releasing peptide receptor (GRPR), also known as bombesin (BBN) receptor subtype II, is a member of the G protein–coupled receptor family of BBN receptors. During the past few decades, GRPR has been found to be overexpressed in various types of cancer, including prostate cancer, breast cancer, colorectal cancer, pancreatic cancer, glioma, lung cancer, ovarian cancers, endometrial cancers, renal cell cancer, and gastrointestinal stromal tumors (1–6).

Glioma is the most common type of primary tumor of the central nervous system. Originating from glial cells, gliomas are further categorized as astrocytoma, oligodendroglioma, or oligoastrocytoma. Astrocytoma is the most dominant type and is further classified into 4 histopathologic grades according to the criteria of the World Health Organization (WHO) (7). The presence of GRPR has been confirmed in various glioma cell lines (8,9). An immunohistochemical-staining study of surgical samples from glioma patients revealed that all samples were GRPR-positive and that, in normal brain tissue, GRPR was detected in neurons but not in glial cells (10). Moreover, several studies on experimental glioma models have confirmed the tumor-inhibition effect of GRPR antagonists (11–13).

In view of these facts, the ability to noninvasively image GRPR expression would be helpful in drug development, patient stratification, and response monitoring, and various GRPR-targeting imaging probes have been developed to fit this purpose (14–16). BBN is an amphibian homolog of mammalian gastrin-releasing peptide (17,18). BBN(7–14), with the amino acid sequence Gln-Trp-Ala-Val-Gly-His-Leu-Met-NH_2, has been labeled with various radionuclides and used extensively to develop molecular probes for imaging GRPR (14,15,19–22). Multiple preclinical studies have demonstrated receptor-specific accumulation of these tracers in GRPR-positive tumors (23,24). Several BBN-related tracers have also entered early clinical studies (25–29).

However, most of the tracers under clinical investigation are labeled with ^{99m}Tc and based on SPECT imaging (25,30–32). Because PET imaging provides higher sensitivity, increased spatial resolution, and the ability to quantify biodistribution and accurately indicate location, effective BBN-based PET tracers are necessary for GRPR-specific imaging and targeted radiotherapy. Several PET tracers have been applied to the imaging of brain tumors, such as ^{18}F-FDG, amino acid derivatives, thymidine nucleoside analogs, and translocator protein–targeting probes (33). In this work, we aimed to apply a GRPR-specific PET tracer, ^{68}Ga-NOTA-Aca-BBN(7–14) (denoted as ^{68}Ga-BBN), to first-in-human studies. The safety of ^{68}Ga-BBN was evaluated, and the absorbed dose was estimated by analyzing the biodistribution profile in healthy volunteers. We also assessed the value of ^{68}Ga-BBN PET/CT in patients with both low-grade and high-grade gliomas.

MATERIALS AND METHODS

^{68}Ga-BBN Preparation

Aca-BBN(7–14) was synthesized using solid-phase Fmoc chemistry by Peptides International. *S*-2-(4-isothiocyanatobenzyl)-1,4,7-triazacyclono-nane-1,4,7-triacetic acid was purchased from Macrocyclics, and 1,4,7-triazacyclononane-1,4,7-triacetic acid *N*-hydroxysuccinimide (NOTA-NHS) ester was obtained from CheMatech. All other chemicals were purchased from Sigma-Aldrich. NOTA-Aca-BBN(7–14) was synthesized according to a procedure published previously (34). The radiolabeling of NOTA-Aca-BBN(7–14) was performed in a sterile hot cell. The precursor NOTA-Aca-BBN(7–14) was dissolved in deionized water to 1 μg/μL and stored at 4°C before use. ^{68}Ga was eluted from a ^{68}Ge/^{68}Ga generator (ITG) using 0.05 M HCl and mixed with 1.25 M NaOAc buffer to adjust the pH to 4.0. The mixture was then directly transferred to a 1-mL plastic tube containing 30 μg of NOTA-Aca-BBN (7–14). After shaking, the mixture was incubated in a heating block at 100°C for 10 min. The reaction mixture was then cooled, dissolved in sterile phosphate-buffered saline, and passed through a 0.22-μm aseptic filtration membrane. Thin-layer liquid chromatography (Bioscan) was used to test the radiochemical purity, with CH_3OH:NH_4OAc (v/v, 1:1) being used as the developing solution. The radiochemical purity of the product was over 97%.

Subjects

The study was registered at clinicaltrials.gov (NCT02520882) and was approved by the Institutional Review Board of Peking Union Medical College Hospital, Peking Union Medical College, Chinese Academy of Medical Sciences, and all subjects gave written informed consent. All procedures were in accordance with the ethical standards of the institutional and national research committees and with the 1964 Helsinki declaration and its later amendments or comparable ethical standards.

Four healthy volunteers (2 male and 2 female; age range, 46–59 y [mean ± SD, 52.3 ± 7.2 y]; weight range, 59.0–75.0 kg [mean, 67.3 ± 6.8 kg]) took part in the study. The exclusion criteria were mental illness, severe liver or kidney disease (serum creatinine level > 3.0 mg/dL [270 μM] or any hepatic enzyme level ≥5 times over the normal upper limit), a severe allergy or hypersensitivity to radiographic contrast material, claustrophobia (unable to accept PET/CT scanning), and pregnancy or breastfeeding. Before and after injection of ^{68}Ga-BBN, safety data were collected, including vital signs (blood pressure, pulse rate, respiratory frequency, and temperature), physical examination, electrocardiography, laboratory parameters (routine blood testing and level of serum alanine aminotransferase, serum albumin, and serum creatinine), and adverse events.

Twelve patients (8 male and 4 female; age range, 5–44 y [mean, 22.8 ± 15.3 y]) with suspected brain glioma as evaluated by contrast-enhanced MRI also took part in the study. All underwent surgical removal of their tumor within 1 wk after ^{68}Ga-BBN PET/CT. The pathologic diagnosis was determined by 2 neuropathologists independently, with consensus reached by review with a third pathologist when there was any discrepancy. The criteria for

the pathologic diagnosis were based on the 2007 edition of the WHO classification (35,36). Table 1 provides details on the patients and their final diagnoses.

Examination Procedures

For the healthy volunteers, immediately before and 24 h after the ^{68}Ga-BBN PET/CT scan we measured blood pressure, pulse rate, respiratory frequency, and temperature and performed routine blood and urine tests as well as tests of liver and kidney function. We noted and analyzed any possible side effects during and within 1 wk after the scan. No specific subject preparation, such as fasting, was requested. After completing the whole-body low-dose CT scan (140 kV, 35 mA, pitch of 1:1, 5-mm thickness with 3-mm gap, 512 × 512 matrix, 70-cm field of view), we intravenously injected 111–148 MBq (3–4 mCi) of ^{68}Ga-BBN and then completed a serial whole-body PET acquisition (from top of skull to middle of femur) using 6 bed positions. The acquisition was 20 s/bed position for the first minute; 40 s/bed position for the 5-, 10-, and 15-min time points; and 2 min/bed position for the 30-, 45-, and 60-min time points.

For the patients, we intravenously injected a 1.85-MBq (0.05 mCi) dose of ^{68}Ga-BBN per kilogram of body weight. A low-dose CT scan (120 kV, 35 mA, 3-mm layer, 512 × 512 matrix, 70-cm field of view) was obtained, followed 30 min after tracer injection by a 10-min PET acquisition covering the whole head of the patient. Two experienced nuclear medicine physicians manually drew regions of interest on the brain lesions for each image using 3-dimensional ellipsoid isocontouring with the assistance of the corresponding CT images. The results were expressed as SUV_{mean} and SUV_{max}.

Data Analysis and Dosimetry Calculation

The PET images were processed on an MMWP workstation (Siemens). General biodistribution and temporal and intersubject stability were determined by visual analysis. Volumes of interest for normal organs and the concerned lesions were drawn on the serial images, and the radioactivity concentrations and SUVs in these volumes of interest were obtained using the workstation software.

Dosimetry was calculated according to the European Association of Nuclear Medicine dosimetry guidance (37) and a previously reported procedure (38). Non–decay-corrected time–activity curves based on SUVs were generated for each organ. The SUVs were then converted to MBq/MBq on the basis of organ weights from the adult male phantom (73.7-kg body weight) and the adult female phantom (56.9-kg body weight) provided by OLINDA/EXM (version 1.1, Vanderbilt University) (39,40). The time-integrated activity coefficient (residence time) of each organ was determined by fitting the data using a biphasic exponential model included in the software. The residence time of urine in the bladder was calculated by the trapezoidal method using Prism (version 4.0, GraphPad Software, Inc.). The void time was set as 60 min. “Remainder of body” was calculated for each time point as the decayed value of the originally injected activity minus the activity in the source organs and urinary bladder. Effective dose was calculated by entering the time-integrated activity coefficient for the source organs into OLINDA/EXM for either a 73.7-kg male adult or a 56.9-kg female adult.

Immunohistochemical Staining of GRPR

Tumor samples were fixed with 10% neutral buffered formalin and embedded in paraffin. After deparaffinization and rehydration, 5-μm-thick tissue sections were treated with 3% H_2O_2 for 20 min to block endogenous peroxidase. The sections were then washed 3 times with phosphate-buffered saline and briefly in a buffer containing 1% polymerized bovine serum albumin and incubated with rabbit antihuman poly-clonal antibody against GRPR (PA5–256791; Thermo Fisher Scientific). After being washed with phosphate-buffered saline, each section was incubated with horseradish peroxidase–conjugated antirabbit IgG for 60 min at room temperature. Diaminobenzidine was used as the chromogen, and hematoxylin and eosin counterstaining was performed. The stained slides were examined using a light microscope (BX41; Olympus). For semiquantification of GRPR expression, 5 entire high-power fields (×40) containing clusters of malignant cells were identified randomly per slide and scored for intensity and percentage of GRPR staining. The procedure was repeated by 2 independent, experienced examiners.

RESULTS

Safety and Biodistribution

No subjective effects were reported by any of the healthy volunteers or patients after injection of ^{68}Ga-BBN. No adverse events or obvious changes in vital signs or clinical laboratory test results occurred after injection.

Table 2 shows the biodistribution of ^{68}Ga-BBN in healthy volunteers. It cleared quickly through the kidneys, with 17.3% ± 1.35% of the total injected radioactivity observed in the urine at 30 min after injection. Accumulation was highest in the pancreas, with an SUV_{mean} of 17.15 ± 3.00 at 30 min after injection because of the high expression of GRPR (41). The spleen and liver had moderate uptake, with respective SUVs of 1.58 ± 0.36 and 1.43 ± 0.26 at 30 min after injection. Uptake was quite low in the skeleton, lungs, mediastinum, and thorax, including the breast. In particular, the brain had a very low background signal, which facilitated lesion detection (Fig. 1).

Absorbed Dose

Table 3 shows the estimated absorbed dose of ^{68}Ga-BBN for each organ as derived from PET/CT images of healthy volunteers. Because of the high accumulation of radioactivity in the urinary bladder, it had the highest absorbed dose: 0.307 ± 0.356 mSv/MBq. Radioactivity in the urinary bladder also affected neighboring organs such as the uterus and testes, which showed relatively higher absorbed doses than the other organs. The whole-body absorbed dose was 0.00150 ± 0.00029 mSv/MBq, with an effective dose of 0.0276 ± 0.0066 mSv/MBq.

^{68}Ga-BBN PET/CT

All 12 patients in this study had at least one brain lesion as diagnosed by MRI, and ^{68}Ga-BBN PET/CT identified all 14 lesions in the 12 patients. All patients underwent open surgery within 1 wk after PET/CT, and glioma was confirmed in all by the final pathologic evaluation: WHO grade I optic pathway glioma in three, WHO grade I ventricular

ganglioglioma in one, WHO grade II supratentorial glioma in three, WHO grade III supratentorial glioma in three, and WHO grade IV glioblastoma multiforme in two (Table 3).

At 30 min after administration of ^{68}Ga-BBN, all lesions showed prominent tracer accumulation with excellent contrast from surrounding normal brain tissue. The lesion location matched that on MRI well. In some cases, signal intensity within the tumor area was heterogeneous (Fig. 2). Quantitative analysis gave an SUV_{max} and SUV_{mean} of 2.08 ± 0.58 and 1.32 ± 0.37, respectively, for the 14 lesions. Tumor-to-background ratios based on SUV_{max} and SUV_{mean} were 24.0 ± 8.85 and 13.4 ± 4.54, respectively. No significant difference in SUV was found between lesions of different WHO grades.

Correlation with GRPR Expression

Immunohistochemical staining showed positive GRPR expression in all 14 glioma samples (Fig. 2). As shown in Figure 3, there was a significant positive correlation between SUV from ^{68}Ga-BBN PET/CT and expression level of GRPR ($r^2 = 0.71$, $P < 0.001$, for SUV_{max} and $r^2 = 0.54$, $P < 0.01$, for SUV_{mean}).

DISCUSSION

^{68}Ga is a positron-emitting radionuclide produced by a generator rather than a cyclotron. An in-house ^{68}Ge/^{68}Ga generator offers high positron yield (89%), easy access, and low cost (42). Because of the 67.6-min physical half-life of ^{68}Ga, patients may be exposed to less radiation with ^{68}Ga than with longer-lived PET isotopes, but overall radiation exposure is also affected by biologic half-life, distribution profile, and positron energy. Our study found ^{68}Ga-BBN to be safe and well tolerated in all subjects. The 130-MBq typically administered activity of ^{68}Ga-BBN resulted in a whole-body effective dose of 3.58 mSv, which is much lower than the limit set by the Food and Drug Administration (43). In healthy volunteers, a bladder void time of 60 min was assumed for dosimetry calculations, and in glioma patients, a 30-min time point was used for PET acquisition. If a 30-min void time were to be used, the whole-body dose would decrease dramatically. All these data confirm the safety of ^{68}Ga-BBN for further clinical applications.

Sharing the same sequence as the C-terminal region of human GRPR, BBN(7–14) has been extensively investigated in preclinical studies to visualize GRPR expression (16,44,45). In all healthy volunteers, we observed rapid renal clearance and extremely low tracer uptake in normal brain tissue, which facilitates lesion detection. Indeed, all gliomas showed good uptake of ^{68}Ga-BBN, with tumor-to-nontumor ratios of 24.0 ± 8.85. The high pancreas uptake until 60 min indirectly confirms the specificity of ^{68}Ga-BBN. The low uptake in normal brain tissue indicates that ^{68}Ga-BBN cannot penetrate the blood–brain barrier, but the relatively high accumulation of ^{68}Ga-BBN within tumors does suggest disruption of the blood–brain barrier. However, the exact weighting of blood–brain barrier disruption on tracer uptake needs further investigation. Another issue of BBN-based tracers is metabolic stability (29). With the same peptide sequence, we have confirmed that around 20% of tracer remains intact in the circulation at 60 min after injection and that around 50% of intact tracer

is found within tumors (18). To minimize the interference of metabolites in lesion detection and data interpretation, we chose the 30-min time point for image acquisition.

GRPR was detected in all glioma samples, as is consistent with the pathologic findings reported previously (10). ^{68}Ga-BBN accumulation was higher in all these GRPR-positive tumors than in the surrounding normal brain tissues. In addition, the PET-determined SUVs correlated significantly with GRPR expression as evaluated by immunohistochemical staining (Fig. 3). Previously, in a study of dynamic PET imaging using ^{68}Ga-BBN and compartmental analysis in 7 patients with recurrent glioma, Strauss et al. found that the parameter k_1 correlates with expression of GRPR based on gene array data (46). We can reasonably predict that besides being used for lesion detection, ^{68}Ga-BBN PET will be useful as a noninvasive marker to evaluate GRPR expression for patient screening before GRPR-targeted therapy. ^{68}Ga-BBN PET will also be useful to guide drug development and monitor therapy response.

Clear definition of the tumor–nontumor margin is important because the extent of tumor resection is a proven independent factor in overall survival, especially for high-grade glioma. Biopsy and postmortem studies have shown that gliomas extend farther than can be determined using conventional imaging techniques such as CT and MRI (47). Currently, 5-aminolevulinic acid fluorescence is widely used for intraoperative guidance in high-grade-glioma surgery. However, low uptake in low-grade glioma and a high negative predictive value in glioblastoma multiforme are major drawbacks of this strategy (48). In one study (10), ^{68}Ga-BBN showed high uptake by both high- and low-grade gliomas because positive GRPR staining was prevalent in patient tumor samples of both high- and low-grade gliomas and uptake in normal brain was low (SUV, 0.10 6 0.03). Positive GRPR staining was also confirmed in all tumor samples of the current study. Therefore, it is highly probable that ^{68}Ga-BBN PET can be applied to delineate tumor from surrounding normal brain tissue. This tracer might also be used to differentiate radiation-induced necrosis from real progression or recurrence of glioma. All these potential applications warrant further investigation of ^{68}Ga-BBN PET in glioma patients.

CONCLUSION

^{68}Ga-BBN is a safe PET tracer with a favorable biodistribution and dosimetry profile. ^{68}Ga-BBN PET has potential value in both high-grade glioma and low-grade glioma as a biomarker of GRPR expression. Noninvasive PET/CT using ^{68}Ga-BBN is expected to play a part in lesion detection, patient screening, and therapy response monitoring of GRPR-targeted therapy.

Acknowledgments

DISCLOSURE

This work was supported by the Intramural Research Program of the National Institute of Biomedical Imaging and Bioengineering, National Institutes of Health. No potential conflict of interest relevant to this article was reported.

REFERENCES

1. Ananias HJ, van den Heuvel MC, Helfrich W, de Jong IJ. Expression of the gastrin-releasing peptide receptor, the prostate stem cell antigen and the prostate-specific membrane antigen in lymph node and bone metastases of prostate cancer. Prostate. 2009; 69:1101–1108. [PubMed: 19343734]
2. Yang M, Gao H, Zhou Y, et al. ^{18}F-labeled GRPR agonists and antagonists: a comparative study in prostate cancer imaging. Theranostics. 2011; 1:220–229. [PubMed: 21544226]
3. Markwalder R, Reubi JC. Gastrin-releasing peptide receptors in the human prostate: relation to neoplastic transformation. Cancer Res. 1999; 59:1152–1159. [PubMed: 10070977]
4. Reubi JC, Körner M, Waser B, Mazzucchelli L, Guillou L. High expression of peptide receptors as a novel target in gastrointestinal stromal tumours. Eur J Nucl Med Mol Imaging. 2004; 31:803–810. [PubMed: 14985869]
5. Heuser M, Schlott T, Schally A, et al. Expression of gastrin releasing peptide receptor in renal cell carcinomas: a potential function for the regulation of neoangiogenesis and microvascular perfusion. J Urol. 2005; 173:2154–2159. [PubMed: 15879878]
6. Fleischmann A, Waser B, Reubi JC. Overexpression of gastrin-releasing peptide receptors in tumor-associated blood vessels of human ovarian neoplasms. Cell Oncol. 2007; 29:421–433. [PubMed: 17726264]
7. Brat DJ, Prayson RA, Ryken TC, Olson JJ. Diagnosis of malignant glioma: role of neuropathology. J Neurooncol. 2008; 89:287–311. [PubMed: 18712282]
8. Farias CB, Lima RC, Lima LO, et al. Stimulation of proliferation of U138-MG glioblastoma cells by gastrin-releasing peptide in combination with agents that enhance cAMP signaling. Oncology. 2008; 75:27–31. [PubMed: 18719351]
9. Sharif TR, Luo W, Sharif M. Functional expression of bombesin receptor in most adult and pediatric human glioblastoma cell lines: role in mitogenesis and in stimulating the mitogen-activated protein kinase pathway. Mol Cell Endocrinol. 1997; 130:119–130. [PubMed: 9220028]
10. Flores DG, Meurer L, Uberti AF, et al. Gastrin-releasing peptide receptor content in human glioma and normal brain. Brain Res Bull. 2010; 82:95–98. [PubMed: 20211708]
11. Pinski J, Schally AV, Halmos G, Szepeshazi K, Groot K. Somatostatin analogues and bombesin/gastrin-releasing peptide antagonist RC-3095 inhibit the growth of human glioblastomas in vitro and in vivo. Cancer Res. 1994; 54:5895–5901. [PubMed: 7954420]
12. Kiaris H, Schally AV, Sun B, Armatis P, Groot K. Inhibition of growth of human malignant glioblastoma in nude mice by antagonists of bombesin/gastrin-releasing peptide. Oncogene. 1999; 18:7168–7173. [PubMed: 10597318]
13. de Oliveira MS, Cechim G, Braganhol E, et al. Anti-proliferative effect of the gastrin-release peptide receptor antagonist RC-3095 plus temozolomide in experimental glioblastoma models. J Neurooncol. 2009; 93:191–201. [PubMed: 19129973]
14. Carlucci G, Kuipers A, Ananias H, et al. GRPR-selective PET imaging of prostate cancer using [^{18}F]-lanthionine-bombesin analogs. Peptides. 2015; 67:45–54. [PubMed: 25797109]
15. Chen X, Park R, Hou Y, et al. microPET and autoradiographic imaging of GRP receptor expression with ^{64}Cu-DOTA-[Lys^{3}]bombesin in human prostate adenocarcinoma xenografts. J Nucl Med. 2004; 45:1390–1397. [PubMed: 15299066]
16. Garrison JC, Rold TL, Sieckman GL, et al. In vivo evaluation and small-animal PET/CT of a prostate cancer mouse model using ^{64}Cu bombesin analogs: side-by-side comparison of the CB-TE2A and DOTA chelation systems. J Nucl Med. 2007; 48:1327–1337. [PubMed: 17631556]
17. Reubi JC, Mäcke HR, Krenning EP. Candidates for peptide receptor radiotherapy today and in the future. J Nucl Med. 2005; 46(suppl):67S–75S. [PubMed: 15653654]
18. Zhang X, Cai W, Cao F, et al. ^{18}F-labeled bombesin analogs for targeting GRP receptor-expressing prostate cancer. J Nucl Med. 2006; 47:492–501. [PubMed: 16513619]
19. Smith CJ, Volkert WA, Hoffman TJ. Radiolabeled peptide conjugates for targeting of the bombesin receptor superfamily subtypes. Nucl Med Biol. 2005; 32:733–740. [PubMed: 16243649]
20. Prasanphanich AF, Nanda PK, Rold TL, et al. [^{64}Cu-NOTA-8-Aoc-BBN(7–14) NH_2] targeting vector for positron-emission tomography imaging of gastrin-releasing peptide receptor-expressing tissues. Proc Natl Acad Sci USA. 2007; 104:12462–12467. [PubMed: 17626788]

21. Mansi R, Wang X, Forrer F, et al. Development of a potent DOTA-conjugated bombesin antagonist for targeting GRPr-positive tumours. Eur J Nucl Med Mol Imaging. 2011; 38:97–107. [PubMed: 20717822]
22. Pourghiasian M, Liu Z, Pan J, et al. ^{18}F-AmBF 3-MJ9: a novel radiofluorinated bombesin derivative for prostate cancer imaging. Bioorg Med Chem. 2015; 23:1500–1506. [PubMed: 25757604]
23. Kunstler J-U, Veerendra B, Figueroa SD, et al. Organometallic ^{99m}Tc(III) '41 1' bombesin (7–14) conjugates: synthesis, radiolabeling, and in vitro/in vivo studies. Bioconjug Chem. 2007; 18:1651–1661. [PubMed: 17663527]
24. Chatalic KL, Franssen GM, Van Weerden WM, et al. Preclinical comparison of Al^{18}F- and ^{68}Ga-labeled gastrin-releasing peptide receptor antagonists for PET imaging of prostate cancer. J Nucl Med. 2014; 55:2050–2056. [PubMed: 25413139]
25. Van de Wiele C, Dumont F, Dierckx RA, et al. Biodistribution and dosimetry of ^{99m}Tc-RP527, a gastrin-releasing peptide (GRP) agonist for the visualization of GRP receptor-expressing malignancies. J Nucl Med. 2001; 42:1722–1727. [PubMed: 11696645]
26. Van de Wiele C, Phonteyne P, Pauwels P, et al. Gastrin-releasing peptide receptor imaging in human breast carcinoma versus immunohistochemistry. J Nucl Med. 2008; 49:260–264. [PubMed: 18199617]
27. Nock B, Maina T. Tetraamine-coupled peptides and resulting ^{99m}Tc-radioligands: an effective route for receptor-targeted diagnostic imaging of human tumors. Curr Top Med Chem. 2012; 12:2655–2667. [PubMed: 23339761]
28. Ananias HJ, Yu Z, Dierckx RA, et al. ^{99m}technetium-HYNIC (tricine/TPPTS)-Aca-bombesin(7–14) as a targeted imaging agent with microSPECT in a PC-3 prostate cancer xenograft model. Mol Pharm. 2011; 8:1165–1173. [PubMed: 21699202]
29. Ananias HJ, Yu Z, Hoving HD, et al. Application of 99m technetium-HYNIC (tricine/TPPTS)-aca-bombesin (7–14) SPECT/CT in prostate cancer patients: a first-in-man study. Nucl Med Biol. 2013; 40:933–938. [PubMed: 23891351]
30. Van de Wiele C, Dumont F, Broecke RV, et al. Technetium-99m RP527, a GRP analogue for visualisation of GRP receptor-expressing malignancies: a feasibility study. Eur J Nucl Med. 2000; 27:1694–1699. [PubMed: 11105826]
31. Scopinaro F, Varvarigou A, Ussof W, et al. Technetium labeled bombesin-like peptide: preliminary report on breast cancer uptake in patients. Cancer Biother Radiopharm. 2002; 17:327–335. [PubMed: 12136525]
32. Scopinaro F, Varvarigou A, Ussof W, et al. Breast cancer takes up ^{99m}Tc bombesin: a preliminary report. Tumori. 2002; 88(suppl):S25–S28. [PubMed: 12365377]
33. Galldiks N, Langen KJ, Pope WB. From the clinician's point of view: what is the status quo of positron emission tomography in patients with brain tumors? Neuro-Oncol. 2015 Jun 30. [Epub ahead of print].
34. Liu Z, Niu G, Wang F, Chen X. ^{68}Ga-labeled NOTA-RGD-BBN peptide for dual integrin and GRPR-targeted tumor imaging. Eur J Nucl Med Mol Imaging. 2009; 36:1483–1494. [PubMed: 19360404]
35. Louis DN, Ohgaki H, Wiestler OD, et al. The 2007 WHO classification of tumours of the central nervous system. Acta Neuropathol (Berl). 2007; 114:97–109. [PubMed: 17618441]
36. Louis DN, Perry A, Burger P, et al. International Society of Neuropathology-Haarlem consensus guidelines for nervous system tumor classification and grading. Brain Pathol. 2014; 24:429–435. [PubMed: 24990071]
37. Lassmann M, Chiesa C, Flux G, Bardies M. EANM Dosimetry Committee guidance document: good practice of clinical dosimetry reporting. Eur J Nucl Med Mol Imaging. 2011; 38:192–200. [PubMed: 20799035]
38. Zhang J, Lang L, Zhu Z, Li F, Niu G, Chen X. Clinical translation of an albumin-binding PET radiotracer ^{68}Ga-NEB. J Nucl Med. 2015; 56:1609–1614. [PubMed: 26251416]
39. Roivainen A, Kähkönen E, Luoto P, et al. Plasma pharmacokinetics, whole-body distribution, metabolism, and radiation dosimetry of ^{68}Ga bombesin antagonist BAY 86–7548 in healthy men. J Nucl Med. 2013; 54:867–872. [PubMed: 23564761]

40. Wang Z, Zhang M, Wang L, et al. Prospective study of ^{68}Ga-NOTA-NFB: radiation dosimetry in healthy volunteers and first application in glioma patients. Theranostics. 2015; 5:882–889. [PubMed: 26000059]
41. Gonzalez N, Moody TW, Igarashi H, Ito T, Jensen RT. Bombesin-related peptides and their receptors: recent advances in their role in physiology and disease states. Curr Opin Endocrinol Diabetes Obes. 2008; 15:58–64. [PubMed: 18185064]
42. Breeman WA, Verbruggen AM. The ^{68}Ge/^{68}Ga generator has high potential, but when can we use ^{68}Ga-labelled tracers in clinical routine? Eur J Nucl Med Mol Imaging. 2007; 34:978–981. [PubMed: 17333177]
43. Mittra ES, Goris ML, Iagaru AH, et al. Pilot pharmacokinetic and dosimetric studies of ^{18}F-FPPRGD2: a PET radiopharmaceutical agent for imaging αvβ3 integrin levels. Radiology. 2011; 260:182–191. [PubMed: 21502381]
44. Rogers BE, Bigott HM, McCarthy DW, et al. MicroPET imaging of a gastrin-releasing peptide receptor-positive tumor in a mouse model of human prostate cancer using a ^{64}Cu-labeled bombesin analogue. Bioconjug Chem. 2003; 14:756–763. [PubMed: 12862428]
45. Parry JJ, Kelly TS, Andrews R, Rogers BE. In vitro and in vivo evaluation of ^{64}Cu-labeled DOTA-linker-bombesin(7–14) analogues containing different amino acid linker moieties. Bioconjug Chem. 2007; 18:1110–1117. [PubMed: 17503761]
46. Strauss LG, Koczan D, Seiz M, et al. Correlation of the Ga-68-bombesin analog Ga-68-BZH3 with receptors expression in gliomas as measured by quantitative dynamic positron emission tomography (dPET) and gene arrays. Mol Imaging Biol. 2012; 14:376–383. [PubMed: 21744169]
47. Price SJ, Gillard JH. Imaging biomarkers of brain tumour margin and tumour invasion. Br J Radiol. 2011; 84(suppl):S159–S167. [PubMed: 22433826]
48. Roberts DW, Valdés PA, Harris BT, et al. Coregistered fluorescence-enhanced tumor resection of malignant glioma: relationships between δ-aminolevulinic acid-induced protoporphyrin IX fluorescence, magnetic resonance imaging enhancement, and neuropathological parameters. J Neurosurg. 2011; 114:595–603. [PubMed: 20380535]

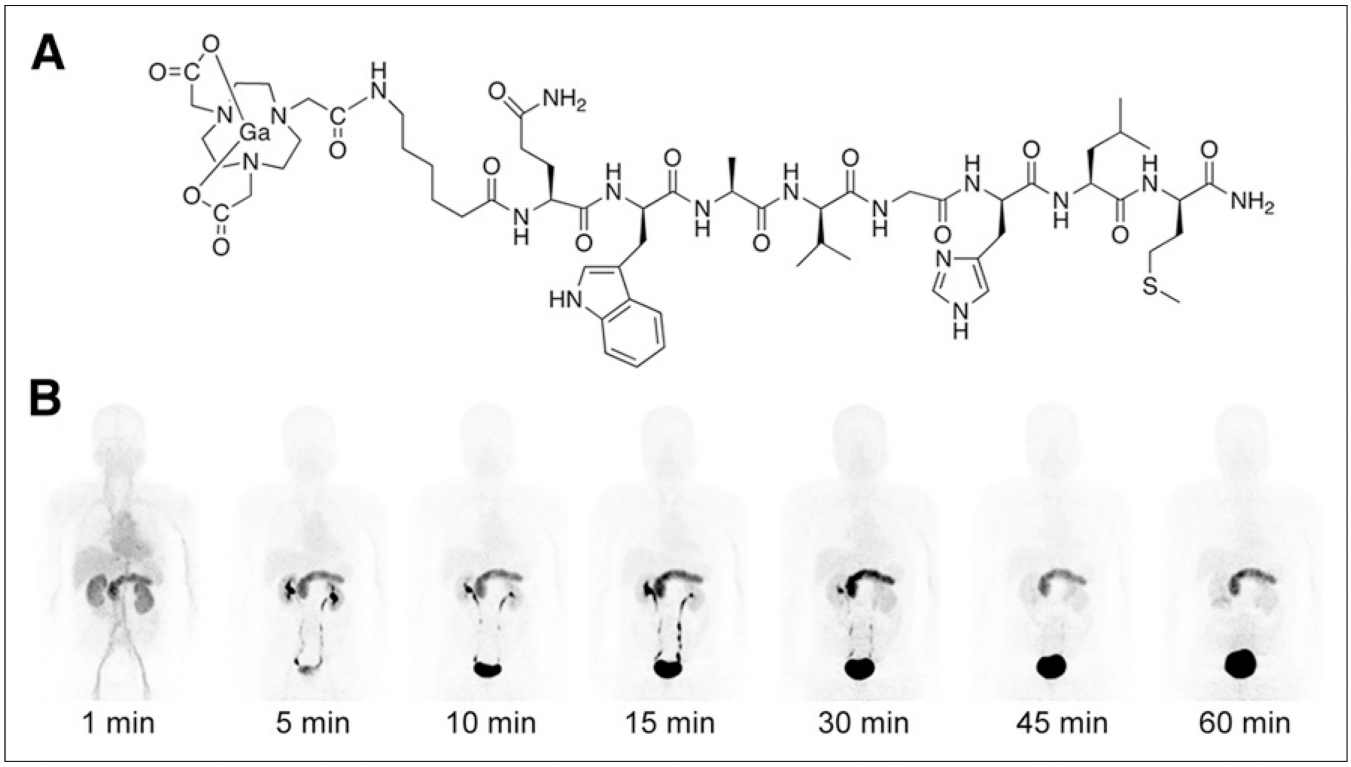

FIGURE 1.

(A) Schematic structure of ^{68}Ga-BBN. (B) Representative maximum-intensity-projection torso images of healthy volunteer at different time points after intravenous injection of ^{68}Ga-BBN. Main regions with prominent ^{68}Ga-BBN uptake are pancreas, kidneys, urinary ducts, and bladder.

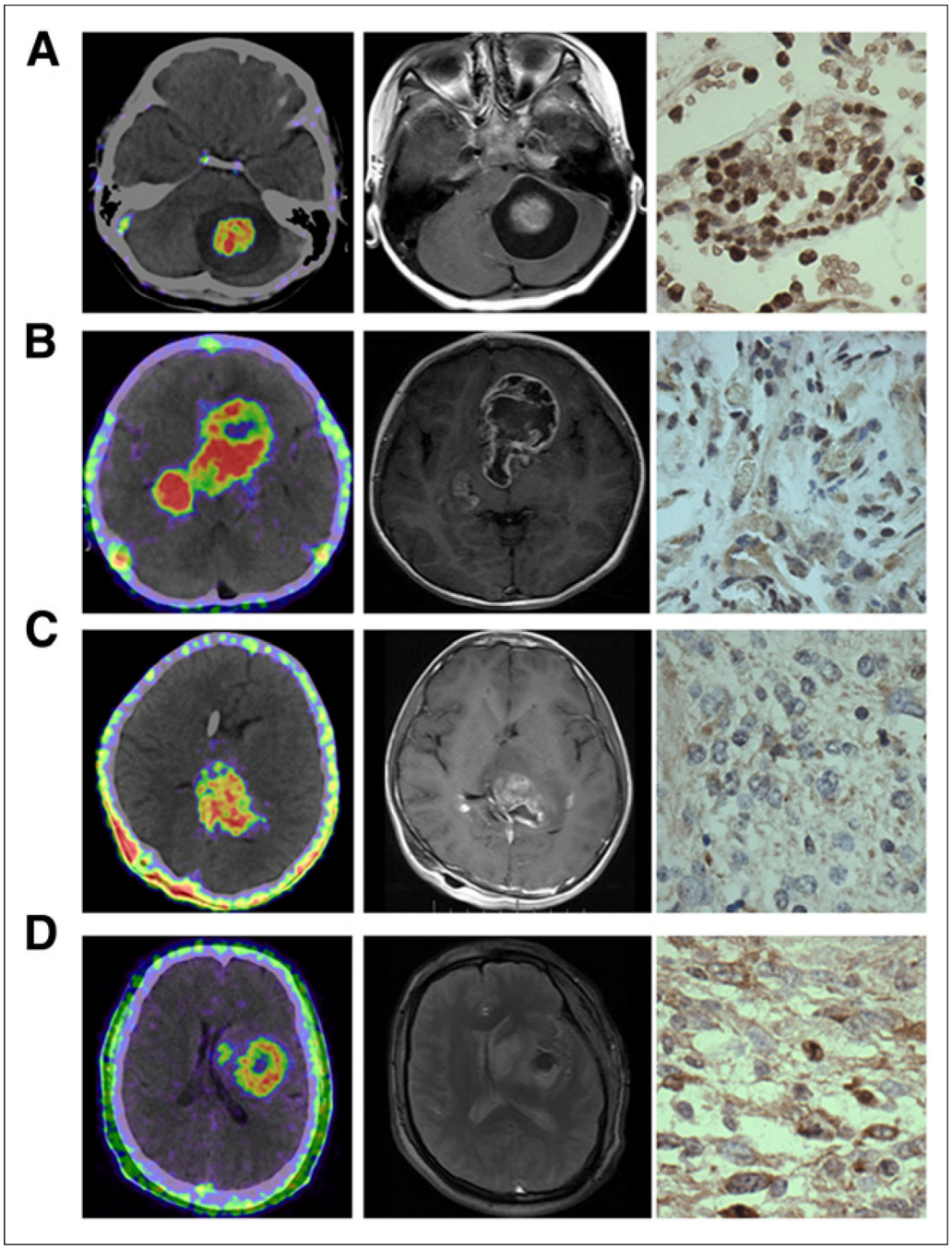

FIGURE 2.

Representative ^{68}Ga-BBN PET/CT images (left), MR images (middle), and immunohistochemically stained tissue samples (right) of patients with gliomas of different grades. (A) A 5-y-old girl with space-occupying lesion in cerebellar lobe diagnosed as pilocytic astrocytoma, WHO grade I. Lesion had SUV_{max} of 2.35 and SUV_{mean} of 1.31, showed enhancement on T1-weighted MRI, and stained positively for GRPR. (B) A 4-y-old girl with multiple space-occupying lesions diagnosed as WHO grade II astrocytoma. Lesions had SUV_{max} of 2.05 and SUV_{mean} of 1.45, were identified by contrast-enhanced T1-

weighted MRI, and stained positively for GRPR. (C) A 14-y-old boy with space-occupying lesion in thalamic connections of temporal lobe diagnosed as WHO grade III anaplastic oligoastrocytoma. Lesion had SUV_{max} of 1.98 and SUV_{mean} of 1.08, showed enhancement on T1-weighted MRI, and stained positively for GRPR. (D) A 44-y-old man with space-occupying lesion in left temporal lobe diagnosed as WHO grade IV glioblastoma multiforme. Lesion had SUV_{max} of 1.95 and SUV_{mean} of 0.98, showed enhancement on T2-weighted MRI, and stained positively for GRPR.

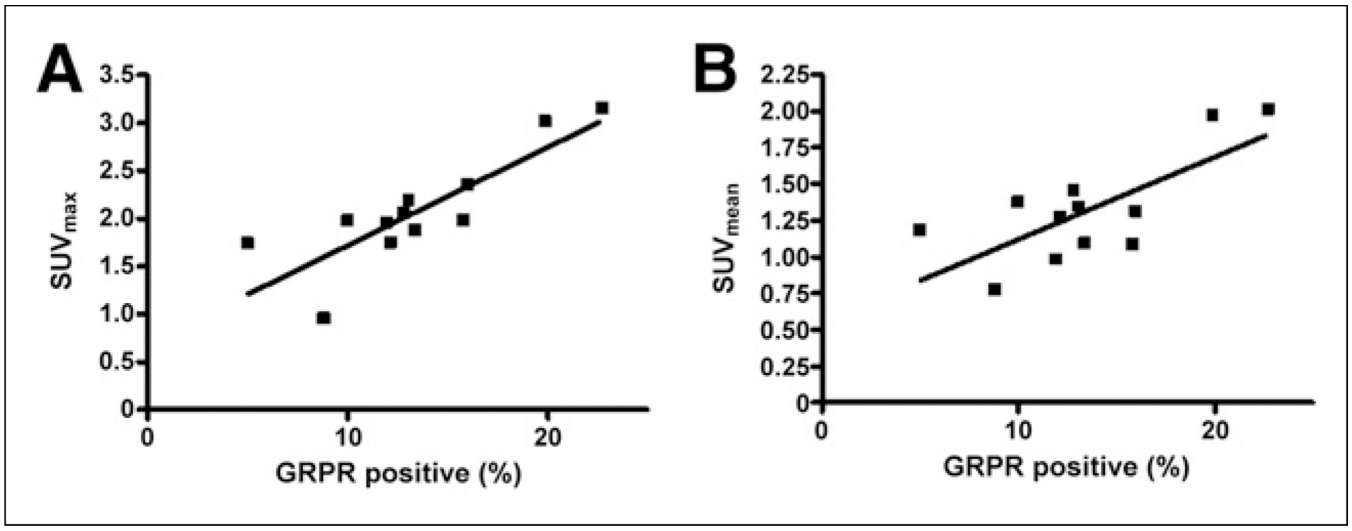

FIGURE 3.

Correlation of SUV_{max} (A) and SUV_{mean} (B) as determined by ^{68}Ga-BBN PET with GRPR expression level as determined by immunohistochemical staining ($r^2 = 0.71$, $P < 0.001$, for SUV_{max} and $r^2 = 0.54$, $P < 0.01$, for SUV_{mean}).

TABLE 1

Patient Demographics

Patient no.	Age (y)	Sex	WHO grade	Histology	Location	MRI findings
1	12	M	I	Ganglioglioma	Third ventricle	Heterogeneous, intense
2	39	M	III	Anaplastic oligoastrocytoma	Right frontal	Heterogeneous, intense
3	14	M	III	Anaplastic oligoastrocytoma	Thalamus, temporal lobe	Heterogeneous, intense
4	4	F	II	Astrocytoma	Seller area	Heterogeneous, intense
5	5	M	II	Pilocytic astrocytoma with necrosis	Seller area	Heterogeneous, moderate
6	5	F	I	Pilocytic astrocytoma	Cerebellar lobe	Heterogeneous, moderate
7	33	F	I	Pilocytic astrocytoma	Seller area	Heterogeneous, intense
8	34	M	III	Anaplastic oligoastrocytoma	Frontal lobe	Heterogeneous, moderate
9	37	M	IV	Glioblastoma multiforme	Frontal lobe	Heterogeneous, intense
10	34	F	II	Oligoastrocytoma	Left frontal	Not applicable
11	12	M	I	Pilocytic astrocytoma	Seller area	Homogeneous, intense
12	44	M	IV	Glioblastoma multiforme	Left temporal lobe	Homogeneous, intense

TABLE 2

Biodistribution of ^{68}Ga-BBN in Healthy Volunteers

	Time (min)						
Organ	**1**	**5**	**10**	**15**	**30**	**45**	**60**
Brain	0.23 ± 0.05	0.18 ± 0.05	0.18 ± 0.05	0.15 ± 0.06	0.15 ± 0.06	0.13 ± 0.05	0.15 ± 0.06
Heart	3.50 ± 0.59	2.88 ± 0.43	2.30 ± 0.23	1.85 ± 0.21	1.60 ± 0.18	1.43 ± 0.22	1.25 ± 0.24
Lung	1.13 ± 0.26	0.81 ± 0.06	0.70 ± 0.08	0.60 ± 0.18	0.50 ± 0.08	0.40 ± 0.08	0.43 ± 0.10
Liver	2.68 ± 0.32	2.18 ± 0.78	1.58 ± 0.21	1.55 ± 0.37	1.43 ± 0.26	1.33 ± 0.26	1.25 ± 0.17
Spleen	2.84 ± 0.30	2.18 ± 0.74	1.65 ± 0.38	1.53 ± 0.43	1.58 ± 0.36	1.50 ± 0.35	1.30 ± 0.35
Pancreas	13.59 ± 2.29	19.79 ± 2.32	20.05 ± 2.11	20.06 ± 4.19	17.15 ± 3.00	13.10 ± 0.14	12.70 ± 2.00
Kidneys	7.73 ± 1.03	6.83 ± 1.26	7.88 ± 3.59	4.88 ± 0.62	3.83 ± 0.63	3.15 ± 0.77	2.70 ± 0.54
Bladder	2.58 ± 1.44	42.67 ± 5.57	74.86 ± 5.51	80.57 ± 5.71	80.30 ± 6.55	75.95 ± 7.23	71.63 ± 5.96
Red marrow	0.50 ± 0.45	0.80 ± 0.24	0.90 ± 0.29	0.85 ± 0.24	0.78 ± 0.24	0.80 ± 0.41	0.73 ± 0.26
Muscle	0.18 ± 0.05	0.48 ± 0.05	0.53 ± 0.10	0.53 ± 0.10	0.45 ± 0.06	0.45 ± 0.06	0.40 ± 0.08

Data are mean SUV ± SD (n = 4).

TABLE 3

Estimated Absorbed ^{68}Ga-BBN Dose in Healthy Volunteers

	mSv/MBq	
Organ	**Mean**	**SD**
Adrenals	0.00021	0.00004
Brain	0.00001	0.00001
Breasts	0.00004	0.00002
Gallbladder wall	0.00053	0.00013
Lower large intestine wall	0.00566	0.00121
Small intestine	0.00228	0.00057
Stomach wall	0.00032	0.00001
Upper large intestine wall	0.00174	0.00044
Heart wall	0.00017	0.00001
Kidneys	0.00058	0.00013
Liver	0.00032	0.00006
Lungs	0.00009	0.00003
Muscle	0.00139	0.00025
Ovaries	0.00530	0.00124
Pancreas	0.00105	0.00015
Red marrow	0.00098	0.00022
Osteogenic cells	0.00058	0.00011
Skin	0.00050	0.00001
Spleen	0.00032	0.00007
Testes	0.01000	—
Thymus	0.00159	0.00177
Thyroid	0.00004	0.00001
Urinary bladder wall	0.30700	0.35559
Uterus	0.01310	—
Total body	0.00150	0.00029
Effective dose equivalent	0.03350	0.00790
Effective dose	0.02760	0.00660